3200 *J. Org. Chem.* **1997,** *62,* 3200−3207

Role of Chelation and Resonance on the Intrinsic Acidity and Basicity of Tropolone

O. Mó,* M. Yáñez, and M. Esseffar[†]

Departamento de Química, C-9, Universidad Autónoma de Madrid, Cantoblanco, E-28049-Madrid, Spain

M. Herreros, R. Notario, and J. L.-M. Abboud*

Instituto Rocasolano, C.S.I.C., C/Serrano, 119, 28006-Madrid, Spain

Received November 19, 1996[⊗]

The gas-phase basicity and acidity of tropolone have been determined by Fourier transform ion cyclotron resonance mass spectrometry (FT ICR) techniques. *Ab initio* calculations at the MP2/-6311+G(d,p) level were carried out to describe the effects that protonation and deprotonation have on the aromaticity and hence on the stability of the system. Experimental and calculated energetics of protonation and deprotonation are in excellent agreement. Our analysis shows that both the protonated and the deprotonated species are stabilized by resonance. As a consequence the acidity of tropolone (341.3 kcal/mol) is enhanced, and this compound is found to be surprisingly as acidic as benzoic acid. This is in good agreement with the results reported in the literature and obtained in DMSO solutions. The intramolecular hydrogen bond becomes significantly weaker upon protonation, and this effect tends to counterbalance the resonance stabilization of the cation. As a consequence, tropolone is found to be slightly less basic than tropone.

Introduction

Molecules having non-benzenoid seven-membered rings have received a great deal of attention regarding their aromaticity.[1] Within this series of compounds tropolone has been extensively studied, both from the experimental and the theoretical points of view,[1−22] notably because it is a medium size molecule which presents an intramolecular hydrogen bond with a symmetric double-minimum potential energy function. Hence, it offers a model system in which to study proton transfer in both the ground and the first excited states.[17,19] Actually, it constitutes a typical example of multidimensional tunneling[22] and there exists experimental evidence showing that at least three fundamental vibrations, namely the OH stretch, carbonyl stretch, and C=C-C stretch, present large tunneling splittings.[14] In spite of this, very little attention was devoted to the role that this intramolecular hydrogen bond or resonance might play in the reactivity of this compound. In this respect, we are only aware of the work of Bordwell and Satish,[23] where the equilibrium acidity in DMSO of tropolone (**1**) is compared to those of benzoic acid and the enol of 1,3-cyclohexadione. These three systems surprisingly have nearly identical acidities ($pK_{HA} = 11.2 \pm 0.2$). This was taken[23] as indicating that the dispersion of the negative charge in the anion rather than the polarity of the carbonyl group is the dominant factor leading to the significant acidity of these systems. These results have prompted us to explore the intrinsic (i.e., solvent-free) acidity and basicity of **1** both experimentally and by means of *ab initio* calculations.

The gas phase basicity of **1**, GB (**1**) is defined as the negative of the Gibbs energy change for reaction 1. The proton affinity, PA (**1**) is the negative of the standard enthalpy change for this reaction:

$$\mathbf{1}(g) + H^+(g) \rightarrow \mathbf{1H}^+(g)(1) \qquad (1)$$

The gas phase acidity of **1** is given by the Gibbs energy change, ΔG_{acid}, for reaction 2:

$$\mathbf{1}(g) \rightarrow \mathbf{1}^-(g) + H^+(g)\ (2) \qquad (2)$$

One of the goals of the present paper is thus to provide both experimental and theoretical information regarding the intrinsic basicity and acidity of tropolone (**1**) as well as to investigate how the intramolecular hydrogen bond and changes in the aromaticity of the system influence both magnitudes. The latter effect can be of importance

---

[†] On leave from the University Cadi Ayyad, Marrakesh, Morocco.

[⊗] Abstract published in *Advance ACS Abstracts*, April 15, 1997.

(1) See for instance Douglase, L. *Non-Benzenoid Conjugated Carbocyclic Compounds. Studies in Organic Chemistry 16*; Elsevier: New York, 1984, and references therein.

(2) Shimanouchi, H.; Sasada, Y. *Acta Crystallogr. B* **1973**, *29*, 81.

(3) Alves, A. C. P.; Hollas, J. M. *Mol. Phys.* **1973**, *25*, 1305.

(4) Redington, R. L.; Redington, T. E. *J. Mol. Spectrosc.* **1979**, *78*, 229.

(5) Brown, R. S.; Tse, A.; Nakashima, T.; Haddon, R. C. *J. Am. Chem. Soc.* **1979**, *101*, 3157.

(6) Rossetti, R.; Brus, L. E. *J. Chem. Phys.* **1980**, *73*, 1546.

(7) Jackman, L. M.; Trewella, T. E.; Haddon, R. C. *J. Am. Chem. Soc.* **1980**, *102*, 2519.

(8) Tomioka, Y.; Ito, M.; Mikami, N. *J. Phys. Chem.* **1983**, *87*, 4401.

(9) Alves, A. C.; Hollas, J. M.; Musa, H.; Ridley, T. *J. Mol. Spectrosc.* **1985**, *109*, 99.

(10) Redington, R. L.; Chen, Y.; Scherer, G. J.; Field, R. W. *J. Chem. Phys.* **1988**, *88*, 627.

(11) Sekiya, H.; Nagashima, Y.; Nishimura, Y. *J. Chem. Phys.* **1990**, *92*, 5761.

(12) Redington, R. L.; Redington, T. E.; Hunter, M. A.; Field, R. W. *J. Chem. Phys.* **1990**, *92*, 6456.

(13) Sekiya, H.; Nishimura, Y.; Li, A. H.; Mori, A.; Takeshita, H. *Chem. Phys. Lett.* **1990**, *173*, 285.

(14) Redington, R. L. *J. Chem. Phys.* **1990**, *92*, 6447.

(15) Kurihara, T.; Ishikawa, S.; Nozoe, T.; Aihara, J. *Bull. Chem. Soc. Jpn.* **1990**, *63*, 2531.

(16) Ríos, M. A.; Rodríguez, J. *Can. J. Chem.* **1991**, *69*, 201.

(17) Tsuji, T.; Sekiya, H.; Nishimura, Y.; Mori, R.; Mori, A.; Takeshita, H. *Chem. Phys.* **1992**, *97*, 6032.

(18) Sekiya, H.; Nagashima, Y.; Tsuji, T.; Nishimura, Y; Mori, A. Takeshita, H. *J. Phys. Chem.* **1991**, *95*, 10311.

(19) Vener, M. V.; Scheiner, S.; Sokolov, N. D. *J. Chem. Phys.* **1994**, *101*, 9755.

(20) Redington, R. L.; Bock, C. W. *J. Phys. Chem.* **1991**, *95*, 10284.

(21) Sanna, N.; Ramondo, F.; Bencivenni, L. *J. Mol. Struct.* **1994**, *318*, 217.

(22) Takada, S.; Nakamura, H. *J. Chem. Phys.* **1995**, *102*, 3977.

(23) Bordwell, F. G.; Satish, A. V. *J. Am. Chem. Soc.* **1994**, *116*, 8885.

S0022-3263(96)02161-5 CCC: $14.00

not only upon deprotonation, as discussed in ref 23, but also upon protonation.

Experimental Section

The gas phase basicity and acidity of **1** were determined from equilibrium proton-transfer reactions conducted in a modified Bruker CMS-47 FT ICR mass spectrometer.[24] Details on this instrument are given in ref 25.

Working conditions were similar to those already described.[26] The average cell temperature is ca. 333 K. These FT ICR measurements provide the standard Gibbs energy change, $\delta\Delta G_{\mathrm{H}^+}(g)$ for the proton-exchange reactions 3 and 4:

$$\mathbf{1}\mathrm{H}^+(g) + \mathrm{B}_{\mathrm{ref}}(g) \rightleftarrows \mathbf{1}(g) + \mathrm{B}_{\mathrm{ref}}\mathrm{H}^+(g) \qquad (3)$$

$$\mathbf{1}(g) + \mathrm{A}^-_{\mathrm{ref}}(g) \rightleftarrows \mathbf{1}^-(g) + \mathrm{AH}_{\mathrm{ref}}(g) \qquad (4)$$

$\mathrm{AH}_{\mathrm{ref}}$ and $\mathrm{B}_{\mathrm{ref}}$ are reference acids and bases, respectively.

For each of these equilibria,

$$\delta\Delta G_{\mathrm{H}^+}(g) = -RT \ln K_p \qquad (5)$$

In every case, the reversibility of reactions 3 and 4 was confirmed by means of double resonance experiments.

In the case of equilibrium 4, $\mathrm{AH}_{\mathrm{ref}}$ and **1** were initially deprotonated by $i\text{-}C_5H_{11}O^-$, generated *in situ* by electron ionization of isoamyl nitrite.

The pressure readings for the various neutral reagents, as determined by the Bayard–Alpert gauge of the FT ICR spectrometer, were corrected by means of the appropriate calibration coefficients obtained by plotting the readings of the ion gauge against the absolute pressures provided by a capacitance manometer (Baratron, MKS). Routinely, three calibration runs were performed on each gas. The reproducibility of the calibration can be estimated at ca. 3%.

Computational Details

The *ab initio* calculations were performed using the Gaussian-94 series of programs.[27] For all compounds included in this study geometry optimizations were carried out initially at the HF/6-31G* level. The corresponding harmonic vibrational frequencies were evaluated at the same level in order to confirm that the optimized structures found correspond to true minima of the potential energy surface and to evaluate the corresponding zero point energy (ZPE) corrections, thermal corrections, and entropy values. The former was scaled by the empirical factor 0.893. A proper description of anions requires, however, to take explicitly into account electron correlation effects and to include diffuse functions in the basis set which are strictly necessary to describe the weakly bound electron of the anion. Hence, the geometry of the deprotonated form of tropolone ($\mathbf{1}^-$) was refined at the MP2(full)/6-31+G(d,p) level. In general, a good description of the geometries of the neutral and the protonated species can be achieved at the MP2(full)/6-31G* level, which is the most common approach used to get optimized geometries for nonanionic systems. However, for the sake of consistency, the geometries of neutral (**1**) and protonated tropolone (**1H**$^+$) were also refined at the MP2/6-31+G(d,p) level. For the latter we have considered the two possible conformations, *cis-trans* (**1H**$^+$) and *trans-trans* (**1H**$^+$**tt**) in order to investigate the role of the intramolecular hydrogen bond on the basicity of the system. It should be mentioned that corroborating our previous arguments, the MP2/6-31+G(d,p)-optimized geometry for the neutral does not differ appreciably from that reported by Sanna et al.[21] at the MP2/6-31G* level. Since the geometries of the protonated and deprotonated forms of tropolone have not been reported so far in the literature, we have included them in Figure 1. This figure also includes the optimized geometry of the tropilium ion (**2**) which will be used in our discussion of the aromaticity of protonated and deprotonated tropolone, as well as that of tropolone itself for the sake of a better discussion of the structural effects produced by the protonation and the deprotonation processes.

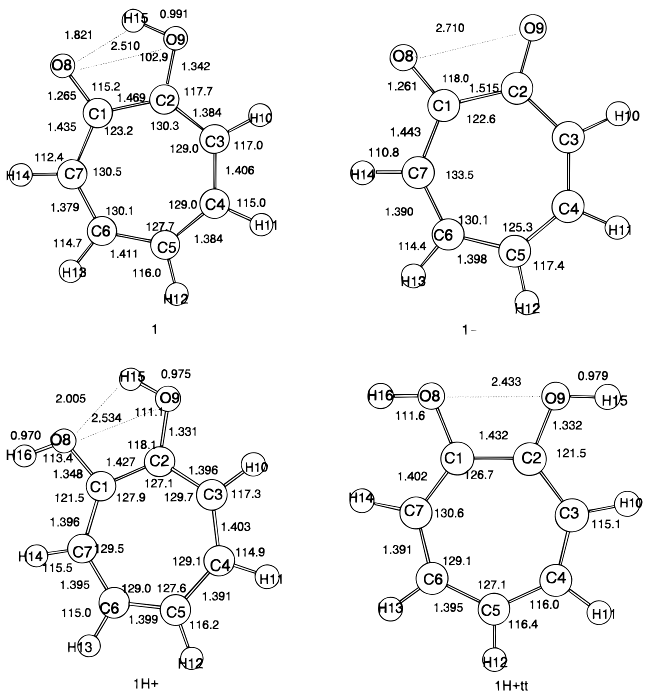

Figure 1. MP2/6-31+G(d,p)-optimized geometries for tropolone (**1**), protonated tropolone (**1H**$^+$, **1H**$^+$**tt**), and deprotonated tropolone ($\mathbf{1}^-$). Bond lengths in angstroms and bond angles in degrees. The C–C and C–H bond lengths for tropilium ion are 1.398 and 1.088 Å, respectively, and the CCC bond angle is equal to 128.6°.

The description of the charge redistributions which take place upon protonation and deprotonation was done in terms of the topological features of the charge densities, $\rho(\mathbf{r})$, and their Laplacians, $\nabla^2\rho(\mathbf{r})$, using the atoms-in-molecules theory of Bader and co-workers.[28–30] For this purpose we have located the bond critical points (bcps) of the species under investigation, i.e., points where the electron charge density hypersurface is minimum

---

[24] *Fourier Transform Mass Spectrometry. Evolution, Innovation and Applications*; Buchanan, M. V., Ed.; ACS Symposium Series 359; American Chemical Society: Washington DC, 1987.

[25] Szulejko, J. E.; McMahon, T. B. *J. Am. Chem. Soc.* **1993**, *115*, 7839.

[26] Abboud, J. L. M.; Herreros, M.; Notario, R.; Esseffar, M.; Mó, O.; Yáñez, M. *J. Am. Chem. Soc.* **1996**, *118*, 1126.

[27] GAUSSIAN-94. Frisch, M. J; Trucks, G. W.; Schlegel, H. B.; Gill, P. M. W.; Johnson, B. G.; Robb, M. A.; Cheeseman, J. R.; Keith, T. A.; Peterson, G. A.; Montgomery, J. A.; Raghavachari, K.; Al-Laham, M. A.; Zakrzewski, M. G.; Ortiz, J. V.; Foresman, J. B.; Cioslowski, J.; Stefanow, B. B.; Nanayaklara, A.; Challacombe, A.; Peng, C. Y.; Ayala, P. Y.; Chen, W.; Wong, M. W.; Andres, J. L.; Replogle, E. S.; Gomperts, R.; Martin, R. L.; Fox, D. J.; Binkley, J. S.; Defrees, D. J.; Baker, J.; Stewart, J. P.; Head-Gordon, M.; Gonzalez, C.; Pople, J. A., (Revision A.1), Gaussian, Inc., Pittsburgh, PA, 1995.

[28] (a) Bader, R. F. W.; Essén, H. *J. Chem. Phys.* **1984**, *80*, 1943. (b) Bader, R. F. W.; MacDougall, P. J.; Lau, C. D. H. *J. Am. Chem. Soc.* **1984**, *106*, 1594.

[29] Bader, R. F. W. *Atoms in Molecules. A Quantum Theory*; Oxford Univ. Press: New York, 1990.

[30] AIMPAC programs package has been provided by J. Cheeseman and R. F. W. Bader.

along the bond path connecting two nuclei of the system and maximum in the other two directions. In particular the values of the electron density and its Laplacian at the critical point would be useful when discussing the characteristics of the intramolecular hydrogen bonds found in tropolone and in its protonated species. The elipticity of the bond is given by $\epsilon = \lambda_2/\lambda_1 - 1$, where λ_1 and λ_2 are the negative curvatures of $\rho(\mathbf{r})$ at the bond critical point.

A comparison of the Laplacian of the charge density of the neutral with those of the corresponding protonated and deprotonated species will provide useful information on the charge redistributions associated with the protonation[31,32] and the deprotonation processes.[33] As it has been shown by Bader et al.[28−30] the Laplacian of the charge density indicates regions of space where the charge density is locally concentrated ($\nabla^2\rho < 0$) or depleted ($\nabla^2\rho > 0$). Hence, a more positive value of the Laplacian of the protonated (or deprotonated) system with respect to the neutral would indicate that electronic charge density has been depleted from that region, while a more negative value of the Laplacian would evidence a charge density concentration in that area.

Since protonation and deprotonation processes may involve substantial hybridization changes not only at the basic or acidic centers, but at other centers of the seven-membered ring, the aforementioned study will be complemented with a NBO analysis,[34] which is also a reliable partition technique to get information on the net atomic charges as well as on the hybridization patterns at each atomic center.

All these population analyses have been carried out on the MP2 densities in order to take into account the electron correlation effects.

The proton affinity (PA) and the intrinsic acidity of tropolone were calculated at the MP2(fc)/6-311+G(d,p) level on the MP2/6-31+G(d,p)-optimized structures. The corresponding total energies are given in Table 1. The ZPE corrections as well as the thermal corrections, which include $^1/_2RT$ for each translational and rotational degree of freedom and the contributions of high vibrational levels were those obtained at the HF/6-31G* level.

Results and Discussion

Structures and Charge Distributions. As mentioned above, the inclusion of diffuse components into the basis set has no dramatic effect on the optimized geometry of tropolone, and our MP2/6-31+G(d,p)-optimized structure is not significantly different from that reported by Sanna et al.[21] at the MP2/6-31G* level. The most significant changes affect the intramolecular hydrogen bond, in the sense that the O···O and the O···H distances found at the MP2/6-31+G(d,p) level are slightly longer (by 0.004 and 0.016 Å, respectively) than those obtained at the MP2/6-31G* level. Another effect of the diffuse components is to enhance the π-delocalization into the troponoid ring, which results in a decrease of the alternation between single and double C−C bond lengths. As shown by Sanna et al.[21] this effect is particularly dramatic when comparing MP2- and HF-optimized structures, which indicates that electron correlation favors π-delocalization. Our results show that this effect is slightly enhanced when the basis set includes diffuse components.

Table 1. Total Energies (*E*, hartrees), Zero Point Energies[a] (ZPE, kcal mol^{-1}), and Entropy Values[b] (S, cal mol^{-1} K^{-1}) for Tropolone (1), Its Protonated (1H$^+$, 1H$^+$tt) and Deprotonated (1$^-$) Species, Tropilium Ion (2), and the Different Compounds Involved in the Homodesmotic Reactions 6−11

compound	E(MP2/ 6-31+G(d,p)	E(MP2/ 6-311+G(d,p)[c]	ZPE	*S*
1	−419.61789	−419.89397	69.71	81.83
1H$^+$	−419.97251[d]	−420.24783	76.85	82.58
1H$^+$tt	−419.88292c[e]	−	76.83	76.78
1$^-$	−419.064121	−419.34089	60.96	83.16
2	−269.89369[e]	−270.02567[f]	71.38	80.75
CH_3COCH_3	−192.60115	−192.72972	50.36	67.21
$CH_3COH^+CH_3$	−192.91839	−193.04764	57.91	71.88
$CH_2{=}COHCH{=}CH_2$	−230.55163	−230.70571	54.39	71.86
$CH_2{=}CO^-CH{=}CH_2$	−229.97744	−230.13039	45.81	70.92
$CH_2{}^+CH{=}CH_2$	−116.59852	−116.66902	41.16	61.10
CH_4	−40.33255	−40.39837	26.77	47.15
$CH_3CH_2CH_3$	−118.74474	−118.82378	61.96	64.93
$CH_3CH{=}CHCH_2{}^+$	−155.81366	−155.91034	57.84	66.91
$CH_3CH{=}CH_2$	−117.44554	−117.60269	47.89	62.76
C_6H_6	−231.53125	−231.69725	60.08	71.39
C_6H_{12}	−235.12877	−235.28497	102.2	73.50
C_4H_{10}(cis)	−157.93232	−158.03755	79.20	72.20
C_4H_8(cis)	−156.71635	−156.81884	64.94	71.48
$C_7H_{13}{}^+$	−273.39283	−273.57126	110.85	81.48

[a] Values obtained at the HF/6-31G* level and scaled by the empirical factor 0.893. [b] Values obtained at the HF/6-31G* level. [c] Values obtained using MP2/6-31+G(d,p)-optimized structures. [d] The MP2/6-31G* value is −419.89094 hartrees. [e] Values obtained at the MP2/6-31G* level. [f] Values obtained using MP2/6-31G*-optimized structures.

Scheme 1

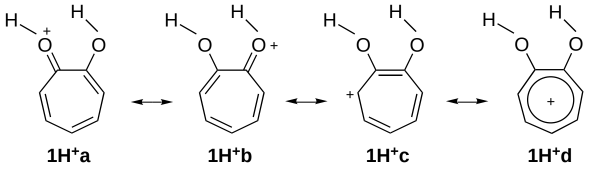

Figure 1 also shows that protonation of tropolone implies significant structural changes: (a) As expected there is a significant lengthening of the C═O bond, since the carbonyl group becomes a C−OH group. (b) The C−OH linkage becomes simultaneously sizeably shorter. (c) There is also a significant shortening of the C1−C2 bond. (d) There is a significant decrease in the alternation between single and double C−C bonds within the ring. (e) The O···O and the O···H distances involved in the intramolecular hydrogen bond increase. As we shall discuss later on, this is consistent with the fact that the intramolecular hydrogen bond in **1H$^+$** is weaker than in **1**.

In principle the valence bond structures given in Scheme 1 should be the most important contributors to the stability of protonated tropolone. However, from the previous structural changes we can infer that **1H$^+$a** form should have a negligible weight, taking into account that both C1−O and C2−C3 bonds significantly lengthen. This is also consistent with the NBO populations since the charge at the protonated oxygen increases slightly, with respect to the neutral system (see Table 2). The shortening of the C−OH bond is consistent with a significant contribution from the mesomeric form **1H$^+$b**. Consistently the hydroxyl oxygen atom becomes more positive

---

(31) Alcamí, M.; Mó, O.; Yáñez, M.; Abboud, J. L. M.; Elguero, J. *Chem. Phys. Lett.* **1990**, *172*, 471.

(32) Abboud, J. L. M.; Notario, R.; Ballesteros, E.; Herreros, M.; Mó, O.; Yáñez, M.; Elguero, J.; Boyer, G.; Claramunt, R. *J. Am. Chem. Soc.* **1994**, *116*, 2486.

(33) Molina, M. T.; Bouab, W.; Esseffar, M.; Herreros, M.; Notario, R.; Abboud, J. L. M.; Mó, O.; Yáñez, M. *J. Org. Chem.*, in press.

(34) Foster, J. P.; Weinhold, F. *J. Am. Chem. Soc.* **1980**, *102*, 7211. Reed, A. E.; Curtiss, L. A.; Weinhold, F. *Chem. Rev.* **1988**, *88*, 899.

Table 2. Atomic Populations Obtained by a NBO Analysis at the MP2/6-311+G(d,p)//MP2/6-31+G(d,p) Level

atomic center	**1**	**1H**$^+$	**1**$^-$
C1	5.660	5.661	5.657
C2	5.672	5.635	6.657
C3	6.232	6.141	6.298
C4	6.162	6.113	6.218
C5	6.184	6.112	6.289
C6	6.176	6.112	6.218
C7	6.190	6.179	6.298
O8	8.604	8.591	8.619
O9	8.648	8.653	8.619
H10	0.508	0.488	–
H11	0.782	0.751	0.818
H12	0.798	0.765	0.831
H13	0.798	0.767	0.828
H14	0.798	0.766	0.831
H15	0.786	0.772	0.818
H16		0.490	–

upon protonation, and the corresponding hydrogen atom becomes more acidic. The contributions of the mesomeric forms **1H**$^+$**c** and **1H**$^+$**d** result in a shortening of the C1–C2 bond. The latter contributor is, however, the most important one, since it is the only one which can account for the fact that the lengths of the C–C bonds of the ring are very similar and not very different from those calculated for tropilium ion (see Figure 1) which can be taken as a prototype of aromatic seven-membered ring system. This strong delocalization of charge in the protonated species with respect to the neutral one is also evidenced by the NBO and Bader analyses. The former technique indicates that the neutral presents alternate single and double C–C bonds, while the protonated species is a highly delocalized system. The topological analysis of the charge densities of these two species does not differ from this description. As shown in Table 3, the charge densities associated with the C2–C3, C4–C5, and C6–C7 as well as their elipticities for the neutral are significantly larger than those of the other C–C bonds of the ring. On the contrary, the charge densities at the C–C bond critical points of species **1H**$^+$ are rather similar. It can be also observed that the elipticities of the C–C bonds of the protonated tropolone become closer. The bonds which were formally single bonds in the neutral increase their elipticity upon protonation due to their higher π character, while those which were formally double bonds in the neutral have a smaller elipticity in the protonated form. This is also mirrored in the characteristics of the Laplacian of its charge density (see Figure 2a) which clearly shows the highly delocalized nature of its charge distribution.

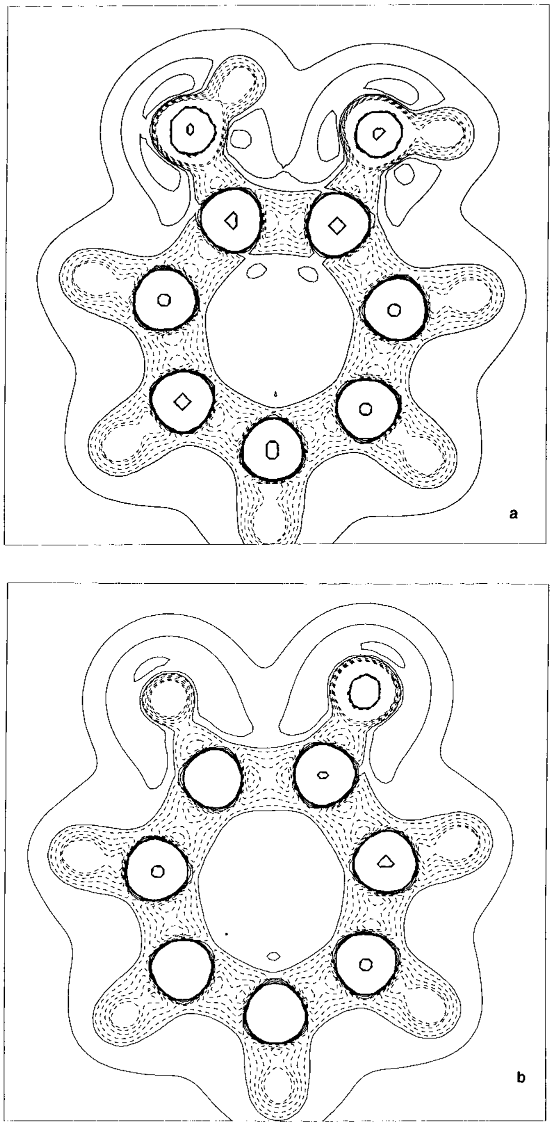

Figure 2. Contour map of the Laplacian of the charge density for (a) protonated tropolone (**1H**$^+$) and (b) deprotonated tropolone (**1**$^-$). Positive values of $\nabla^2\rho$ are denoted by solid lines and negative values by dashed lines. Contour values in au are ±0.05, ±0.12, ±0.25, ±0.37, ±0.50, ±0.62, ±0.75, ±0.80, ±0.95, ±1.00, and ±1.05.

Table 3. Bonding Characteristics of Tropolone and Its Protonated and Deprotonated Derivatives and Tropilium Ion. The Values of ρ and $\nabla^2\rho$ at the bcps Are in au

	1			**1H**$^+$			**1**$^-$			**2**		
bond	ρ	$\nabla^2\rho$	ϵ	ρ	$\nabla^2\rho$	ϵ	ρ	$\nabla^2\rho$	ϵ	ρ	$\nabla^2\rho$	ϵ
C1–C2	0.281	−0.731	0.141	0.303	−0.848	0.206	0.260	−0.641	0.109	0.306	−0.871	0.150
C2–C3	0.320	−0.915	0.248	0.311	−0.889	0.182	0.288	−0.754	0.166			
C3–C4	0.303	−0.824	0.175	0.313	−0.876	0.177	0.309	−0.835	0.243			
C4–C5	0.318	−0.890	0.229	0.310	−0.867	0.156	0.307	−0.837	0.221			
C5–C6	0.301	−0.823	0.159	0.313	−0.877	0.168	0.307	−0.837	0.221			
C6–C7	0.319	−0.893	0.235	0.309	−0.856	0.175	0.309	−0.835	0.243			
C7–C1	0.293	−0.796	0.142	0.313	−0.883	0.214	0.288	−0.754	0.166			
C1–O8	0.367	−0.874	0.062	0.296	−0.263	0.003	0.364	−0.009	0.056			
C2–O9	0.305	−0.276	0.015	0.313	−0.273	0.010	0.364	−0.009	0.056			
O9–H10	0.325	−1.856	0.018	0.340	−2.037	0.017						
C3–H11	0.284	−1.041	0.018	0.288	−1.109	0.009	0.282	−1.007	0.028	0.284	−1.012	0.008
C4–H12	0.285	−1.040	0.017	0.289	−1.107	0.008	0.280	−0.988	0.021			
C5–H13	0.285	−1.040	0.020	0.289	−1.107	0.009	0.281	−0.987	0.040			
C6–H14	0.284	−1.038	0.014	0.289	−1.103	0.009	0.280	−0.988	0.021			
C7–H15	0.285	−1.057	0.015	0.285	−1.059	0.012	0.282	−1.007	0.028			
O8–H16				0.343	−2.032	0.018						

Scheme 2

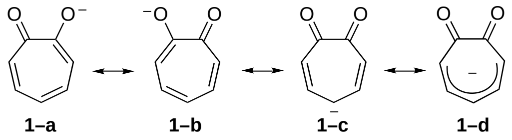

Most importantly, this topological analysis also indicates that the intramolecular hydrogen bond becomes considerably weaker upon protonation. As indicated in Table 3, the charge density at the corresponding bond critical point becomes one-half upon protonation, and consistently both the O···O and the O···H distances become longer. This result is not easy to predict, since protonation has two opposite effects on the strength of the hydrogen bond (HB). On one hand the hydrogen atom involved in the HB becomes more acidic, what should result in an increase of the strength of the linkage. On the other hand, the carbonyl oxygen atom becomes a poorer HB acceptor upon protonation, which should be reflected in a weaker interaction. According to our results it seems clear that the latter effect dominates and the HB of the protonated species is significantly weaker than in the neutral one. As we shall discuss in forthcoming sections, this will have a sizeable effect on the intrinsic basicity of this compound.

The geometry changes upon deprotonation of tropolone are also significant. Let us single out the most significant ones for comment: (a) It can be seen that the bond length of the carbonyl group remains practically unchanged, while as expected, the C–OH bond significantly shortens upon deprotonation. Obviously, both C═O bonds become equivalent by symmetry and have a bond length typical of carbonyl groups. (b) The C1–C2, C2–C3, and C1–C7 linkages lengthen significantly. (c) The remaining C–C bonds of the ring present nearly equal bond lengths and are quite similar to those exhibited by the tropilium ion. (d) The O···O distance significantly increase due to the fact that the stabilization provided by the intramolecular hydrogen bond is replaced by the repulsion between the oxygen lone-pairs. As a consequence the deprotonated species is not strictly planar. The two oxygen atoms are located above and below the plane defined by the seven-membered ring, so that the OCCO dihedral angle is 10.7°. In this respect, it should be mentioned that this effect is only reproduced when including electron correlation effects in the theoretical treatment. At the HF/6-31G* level, the deprotonated species **1**$^-$ is predicted to be a strictly planar C_{2v} structure.

In general, the mesomeric forms depicted in Scheme 2 may contribute to the stability of species **1**$^-$. However points a and b clearly rule out the participation of forms **1**$^-$**a** and **1**$^-$**b**. Consistently the charges at both carbonyl oxygen atoms are slightly smaller than the average in the neutral. Point c clearly indicates that form **1**$^-$**d** must be the most important contributor to the aromatic character of the anionic compound. Again this is clearly reflected in the characteristics of the Laplacian of its charge density (see Figure 2b) and in the fact that the molecular electrostatic potential is attractive all around the molecular system (see Figure 3) which evidences the dispersion of the negative charge within the ring. It is apparent from the values in Table 2 that the natural populations of both oxygen atoms and the carbon atoms directly bonded to them remain practically unchanged upon deprotonation, while the half electron associated to the hydrogen atom, which is removed from the system, is dispersed over the rest of the carbon atoms of the seven-membered ring, whose natural population slightly increases. The fact that the C3–C4 and C6–C7 bonds are slightly shorter than the C5–C6 and C4–C5 linkages is indicative of a certain participation of mesomeric form **1**$^-$**c**. This is in agreement with the NBO analysis which predicts a quite delocalized charge distribution with a certain double bond character for the C3–C4 and C6–C7 linkages. Consistently, the charge densities at the C1–C2, C1–C7, and C2–C3 bond critical points are typical of single C–C bonds, while those of the remaining bonds of the system are larger and similar to those found for tropilium ion (see Table 3). Hence, we must conclude that either protonation or deprotonation of tropolone imply an increase of the aromatic character of the system.

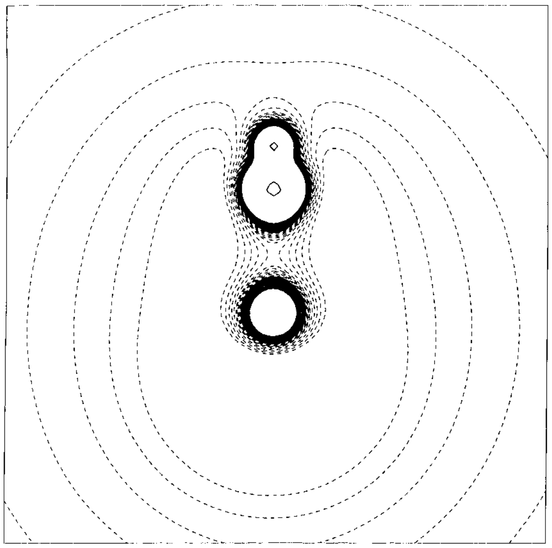

Figure 3. Molecular electrostatic potential map of deprotonated tropolone (**1**$^-$) evaluated in the symmetry plane perpendicular to the ring. Positive and negative values of the potential are denoted by full and dashed lines, respectively. Contour values in kcal/mol are ±1, ±2, ±3, ±4, ±5, ±10, ±15,...

Harmonic Vibrational Frequencies. The HF/6-31G* harmonic vibrational frequencies of species **1**, **1H**$^+$, **1**$^-$, and **2** have been summarized in Table 4. It should be mentioned that the force field of the neutral was already reported in the literature at different levels of accuracy, ranging from HF/4-31G* to MP2/6-31G*, and the frequencies assigned to the different vibrational modes in ref 20, so this section will be devoted almost exclusively to establish the correlations between the vibrational modes of tropolone **1** and those of its protonated **1H**$^+$ and deprotonated **1**$^-$ species. It must be mentioned, however, that the assignments reported in ref 20 were based in HF/6-31G calculations, and we have observed that inclusion of polarization functions lead to changes in the relative frequencies of some vibrational modes. More specifically, the vibrational modes numbered as 7, 8, and 9 in ref 20 correspond to the vibrational modes 9, 7, and 8, respectively, in our case. In other words, the carbonyl stretch (ν_9) in ref 20 is predicted to appear at higher vibrational frequencies (ν_7) when polarization functions are included in the basis set. Similarly, the vibrational modes 12–13 and 15–16 of ref 20 appear in the reversed order at the HF/6-31G* level. Regarding the protonated tropolone **1H**$^+$, values in Table 4 show that the two highest frequency absorptions, corresponding to the O–H stretchings, appear at higher frequencies than the O–H stretch of the neutral. This is consistent with the

Table 4. Calculated Harmonic Vibrational Frequencies (cm^{-1}). For Compounds 1, 1$^-$, and 1H$^+$, the Frequencies Which Correspond to Similar Normal Modes Are Given in the Same Row, Unless Otherwise Indicated by Means of Arrows

1H$^+$	1	1$^-$	2
4070 (a′)			
4021 (a′)	3861 (a′)		
3406 (a′)	3386 (a′)	3336 (a_1,a)	3405 (a_1)
3401 (a′)	3380 (a′)	3328 (b_2,b)	3401 (b_2)
3399 (a′)	3372 (a′)	3323 (a_1,a)	3397 (a_1)
3383 (a′)	3354 (a′)	3273 (b_2,b)	3388 (a_1)
3361 (a′)	3344 (a′)	3268 (a_1,a)	3386 (b_2)
	1887 (a′)	1863 (b_2,b)	3377 (a_1)
1801 (a′)	1858 (a′)	1861 (a_1,a)	3375 (b_2)
1774 (a′)	1828 (a′)	1788 (a_1,a)	1781 (a_1)
1700 (a′)	1666 (a′)	1685 (b_2,b)	1779 (b_2)
1639 (a′)	1648 (a′)	1610 (b_2,b)	1649 (b_2)
1617 (a′)	1591 (a′)	1600 (a_1,a′)	1648 (a_1)
1559 (a′)	1570 (a′)	1499 (b_2,b)	1613 (a_1)
1514 (a′)	1450 (a′)		1613 (b_2)
1487 (a′)	1418 (a′)	1485 (a_1,a)	1567 (b_2)
1449 (a′)			1384 (a_1)
1375 (a′)	1382 (a′)	1339 (b_2,b)	1383 (b_2)
1341 (a′)	1352 (a′)	1334 (a_1,a)	1345 (a_1)
1323 (a′)	1313 (a′)	1282 (b_2,b)	1344 (b_2)
1284 (a′)			1198 (a_2)
1180 (a″)	1155 (a″)	1121 (a_2,a)	1198 (b_1)
1163 (a″)	1134 (a″)	1104 (b_2,b)	1175 (a_2)
1151 (a′)	1134 (a′)	1100 (b_1,b)	1174 (b_1)
1082 (a″)	1033 (a″)	1053 (a_1,a)	1084 (b_2)
1063 (a′)	1028 (a′)	959 (a_1,a)	1083 (a_1)
984 (a″)	957 (a″)	936 (a_2,a)	981 (b_1)
945 (a′)	947 (a′)	905 (b_1,b)	980 (a_2)
850 (a″)	865 (a″)	821 (a_2,a)	942 (a_1)
782 (a″)	805 (a′)	815 (b_2,b)	941 (b_2)
773 (a′)	783 (a″)	773 (b_1,b)	938 (a_1)
741 (a′)	723 (a′)	701 (a_1,a)	732 (b_1)
627 (a″)	660 (a″)		607 (b_1)
577 (a″)	624 (a″)	659 (b_1,b)	697 (a_2)
561 (a′)	586 (a′)	586 (b_2,b)	469 (a_1)
485 (a′)	479 (a′)	479 (a_1,a)	469 (b_2)
437 (a″)	448 (a″)	451 (b_1,b)	248 (b_1)
399 (a″)	402 (a′)	427 (a_2,a)	248 (a_2)
397 (a′)	387 (a′)	389 (a_1,a)	
394 (a′)	379 (a″)	380 (b_2,b)	
379 (a″)			
201 (a″)	202 (a″)	161 (b_1,b)	
124 (a″)	97 (a″)	50 (a_2,a)	

topology of the electron charge densities, which shows that the values of $\rho(\mathbf{r})$ at the O−H bcps are higher in the protonated species than in the neutral. This is also coherent with the fact, mentioned above, that the intramolecular hydrogen bond is weaker in the former. It is also apparent that all C−H stretches are blue-shifted upon protonation. The absorption predicted at 1887 cm^{-1} for the neutral has no equivalent in the protonated species, since it corresponds to the carbonyl stretch. The C−OH stretch in the neutral contributes to several absorptions, those predicted at 1858, 1591, 1450, and 1418 cm^{-1}, respectively. For the protonated species, the C−OH stretches contribute essentially to the 1801, 1487, and 1449 cm^{-1} absorptions. The absorption found at 1449 cm^{-1} corresponds to the C−OH stretch associated with the protonated carbonyl group and therefore has no equivalent in the neutral species. Consistently with the fact that both C−OH groups have different local geometries, with different C−O bond lengths and different charge densities at the corresponding bcps (see Table 3), their stretches have different frequencies. The bands predicted at 1284 cm^{-1} and 379 cm^{-1}, which have no correspondence in the neutral are assigned to the in-plane and out-of-plane bending motions of the protonated carbonyl group, respectively.

Table 5. Resonance Energies (ΔE_r, (kcal/mol) Associated with the Homodesmotic Reactions 6−11. Values Obtained at the MP2/6-311+G(d,p)//MP3/6-31G* Level, after Including ZPE Corrections

reaction	ΔE_r	reaction	ΔE_r
6	66.0	9	57.5
7	42.3	10	48.7
8	34.6	11	67.8

Regarding the harmonic vibrational frequencies of species **1**$^-$, it must be recalled here that at the HF/6-31G* level this system is predicted to have C_{2v} symmetry, while at the MP2/6-31+G(d,p) level it adopts a C_2 structure. Hence, in Table 4 we have indicated the C_{2v} irreducible representation to which each normal mode belongs, as well as the symmetry which each of them would have for a C_2 symmetry system. Quite importantly, taking into account that all a_2 vibrational modes are infrared inactive, and that in the C_2 arrangement of species **1**$^-$ both oxygen atoms are only slightly out of the plane of the ring, it can be reasonably assumed that all vibrations of the C_2 structure which correlate with a_2 modes of the C_{2v} form should have negligible intensities.

Contrarily to what is predicted for the protonation of tropolone, its deprotonation implies a red shifting of the C−H stretching displacements. The carbonyl stretchings appear as symmetric and asymmetric combinations, at 1863 cm^{-1} and 1861 cm^{-1}, respectively. The absorbtion predicted to appear at 1450 cm^{-1} for the neutral has no equivalent in the deprotonated species, since it corresponds essentially to a C−O−H bending. This permits to ratify the assignment made by Redington and Boch[20] in the sense that this is one of the vibrational modes of the neutral which is strongly affected by the intramolecular hydrogen bond.

Resonance Energies. In order to quantify the changes in the aromatic character of the tropolone system upon protonation and deprotonation, we have considered it of interest to evaluate the resonance energy of each of these species by means of the appropriate homodesmotic reaction as defined by George et al.,[35] i.e., a reaction where the number and nature of the bonds, as well as the number and hybridization of the different atomic centers, are the same in both sides of the reaction. To have a useful reference we have also estimated the resonance energy of the tropilium ion, which, as we have mentioned above, can be taken as a prototype of aromatic seven-membered ring system and which can be easily compared with benzene.

For tropilium ion

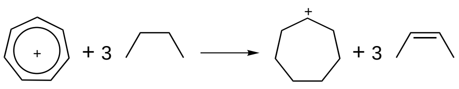

2 (C$_7$H$_{13}$) (6)

the following homodesmotic processes would be a good choice: since it allows a direct comparison with benzene for which a similar homodesmotic reaction would be:

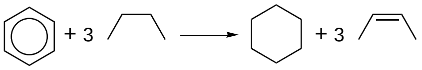

(7)

Unfortunately, similar processes involving seven-membered saturated rings cannot be defined for neither

---

(35) George, P.; Trachtman, M.; Bock, C. W.; Brett, A. M. *J. Chem. Soc., Perkin Trans. 2* **1976**, 1222.

tropolone nor to its protonated and deprotonated species, since these saturated rings are highly unstable or do not exist. Reasonably good alternatives would be reactions 8−10.

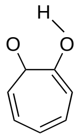

1

$$+ 3CH_4 \longrightarrow CH_3COCH_3 + CH_2{=}COHCH{=}CH_2 + CH_3CH{=}CH_2 \qquad (8)$$

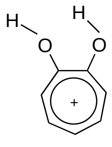

1H⁺

$$+ 3CH_4 \longrightarrow CH_3COH^+CH_3 + CH_2{=}COHCH{=}CH_2 + CH_3CH{=}CH_2 \qquad (9)$$

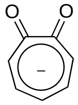

1−

$$+ 3CH_4 \longrightarrow CH_3COCH_3 + CH_2{=}CO^-CH{=}CH_2 + CH_3CH{=}CH_2 \qquad (10)$$

For tropilium ion the equivalent homodesmotic process would be:

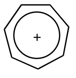

$$+ 3CH_4 \longrightarrow 2CH_3CH{=}CH_2 + CH_3CH{=}CHCH_2^+ \qquad (11)$$

2

The resonance energies were obtained at the MP2/6-311+G(d,p)//MP2/6-31+G(d,p) level, after including the corresponding scaled ZPE corrections evaluated at the HF/6-31G* level. The corresponding total energies and ZPE corrections have been included in Table 1. The calculated resonance energies are presented in Table 5. The first important finding is that the resonance energy estimated for tropilium ion using reactions 6 and 11 are nearly equal, which indicates that reactions 8−10 may be taken as reliable schemes to estimate the resonance energies of tropolone and its protonated and deprotonated species with respect to tropilium ion. It can be also seen that in agreement with our previous discussion both protonated **1H**$^+$ and deprotonated **1**$^-$ tropolone have a resonance energy sizeably larger than the corresponding neutral. Also interestingly, the highest resonance energy corresponds to tropilium ion, which is a typical aromatic system. It is worth noting that this resonance energy is higher than that estimated for benzene. However, this result should be taken with caution because while cyclohexane is a very stable saturated six-membered ring, the $C_7H_{13}^+$ system has a tricoordinated carbon, which may decrease its stability and therefore exaggerate the resonance energy estimated for tropilium ion. The large resonance energy obtained for protonated tropolone indicates that the π-delocalization in this system contributes significantly to the stabilization of the system. A similar effect, although smaller is observed for the deprotonated species, where the π-delocalization, as we have discussed above, does not involve the whole carbon skeleton, but the C3−C4−C5−C6−C7 framework exclusively. These resonance stabilizations have an important influence on the intrinsic basicity and acidity of tropolone.

Table 6. Experimental Determination of the Gas-Phase Basicity of Tropolone. All Values in kcal mol^{-1}

reference	GB(ref)[a]	$\delta\Delta G_{H^+}$	GB	GB(av)	PA[b]
$HCON(CH_3)_2$	203.8	2.47	206.27		
$(t\text{-}C_4H_9)_2S$	206.0	0.24	206.24	206.2	213.7
$H_2C{=}CHCH_2NH_2$	208.5	−2.40	206.10	(sd = 0.1) (208.2)[c]	(216.2)[c]

[a] Values taken from ref 36. [b] Proton affinity calculated from GB value using $T\Delta S$ = 7.5 kcal mol^{-1} (see text). [c] Calculated value obtained at the MP2/6-311+G(d,p) level (see text).

Gas-Phase Basicity and Acidity. Gas Phase Basicity. Table 6 presents the results of the experimental study of the proton-transfer equilibria 1 between **1** and a series of standard reference bases (see reaction 3).

The values of $\delta\Delta G_{H^+}(g)$ given in this table are defined by means of eq 5.

The experimental gas phase basicity of **1**, GB(**1**), is given by GB(av), the average of the negative of the ΔG values obtained for each reference base through eq 12:

$$\Delta G = \delta\Delta G_{H^+}(g) + \Delta G_{H^+}(\text{ref}) \qquad (12)$$

where $\Delta G_{H^+}(\text{ref})$ pertains to reaction 13 and GB(ref) = $-\Delta G_{H^+}(\text{ref})$

$$B_{\text{ref}}(g) + H^+(g) \rightarrow B_{\text{ref}}H^+(g) \qquad \Delta G_{H^+}(\text{ref}) \qquad (13)$$

The values of $\Delta G_{H^+}(\text{ref})$ used in this work have been determined in Prof. Taft's laboratory and are given in ref 36. These values have been anchored to the most recent value[25] of GB(NH_3), namely 195.3 kcal mol^{-1}. As shown in Table 6, this leads to a value of GB(**1**) of 206.2 kcal mol^{-1}.

Inasmuch as the entropy change for reaction 1 cannot be obtained directly from the FT ICR experiments, we have used the value computed at the HF/6-31G**//6-31G** level, namely 0.75 cal mol^{-1} K^{-1}. This value combines the contribution from $S(H^+)$ as determined from the Sackur−Tetrode equation with those from ΔS(rot) and ΔS(vib) for the molecules and ions as determined by means of the partition functions calculated at the HF/6-31G*//6-31G* level. The standard state is 298 K and 1 atm (0.1 MPa). This yields a value of PA(**1**) of 213.7 kcal mol^{-1}.

Gas Phase Acidity. The Gibbs energy change for reaction (2), $\Delta G_{\text{acid}}(\mathbf{1})$ is given by $\Delta G_{\text{acid}}(g)(\text{av})$, the average of the $\Delta G_{\text{acid}}(g)$ values obtained through eq 14:

$$\Delta G_{\text{acid}}(g) = \delta\Delta G_{\text{acid}}(g) + \Delta G_{\text{acid}}(\text{ref}) \qquad (14)$$

wherein $\Delta G_{\text{acid}}(\text{ref})$ pertains to reactions 15:

$$A{-}H_{\text{ref}}(g) \rightarrow A^-_{\text{ref}}(g) + H^+(g) \qquad (15)$$

Values of $\Delta G_{\text{acid}}(\text{ref})$ are taken from ref 37. Experimental results are summarized in Table 7.

From these results we obtain: $\Delta G_{\text{acid}}(\mathbf{1}) = 333 \pm 0.2$ kcal mol^{-1}, the corresponding standard enthalpy change is $\Delta H_{\text{acid}}(\mathbf{1}) = 341.2$ kcal mol^{-1} using the computed (see above) entropy change (1.336 cal mol^{-1} K^{-1}).

Notice that the uncertainties reported for acidities and basicities are rather small, as far as the overlaps with the reference compounds are concerned. The "absolute"

---

(36) Lias, S. G.; Bartmess, J. E.; Liebman, J. F.; Holmes, J. L.; Levin, R. D.; Mallard, W. G. *NIST Standard Reference Database 19A, Positive Ion Energetics Database 1982, Version 1.1*; NIST Standard Reference Data, NIST: Gaithersburg, MD 20899.

Table 7. Experimental Determination of the Gas-Phase Acidity of Tropolone. All Values in kcal mol^{-1}

reference	ΔG_{acid}(ref)^a	$\delta\Delta G_{acid}$	ΔG_{acid}	ΔG_{acid}(av)	ΔH_{acid}^{b}
m-ClC_6H_4OH	335.0	−1.97	333.03		
C_6H_5SH	333.7	−0.62	333.08	333.0	341.2
m-$CF_3C_6H_4OH$	332.4	0.42	332.82	(sd = 0.1) (331.6)^c	(339.8)^c

^{a} Values taken from ref 37. ^{b} Deprotonation enthalpy calculated from ΔG_{acid} value using $T\Delta S = 8.2$ kcal mol^{-1} (see text). ^{c} Calculated value obtained at the MP2/6-311+G(d,p) level (see text).

values are obviously less precise, perhaps by as much as 1 or 2 kcal/mol. The quality is very likely not significantly worst than this, because of the multiple overlaps involved in the construction of the acidity and basicity scales.

As shown in Tables 6 and 7 there is an excellent agreement between calculated and experimental values, which show that tropolone is as acidic in the gas phase as benzoic acid.[37] This is an unexpected result in the light of the theory which postulates that the polarity of the carbonyl group is the dominant factor to explain the acidity of a CO_2H group. As indicated by Bordwell and Satish,[23] tropolone (**1**) can be considered as a vinylogue of benzoic acid, in which three CH═CH groups have been interspersed between the C═O and OH moieties. This would imply necessarily that the acidity of the former should be smaller than that of the latter. However our results, in agreement with previous findings in solution,[23] show that both compounds have the same acidity. This clearly ratifies our previous arguments in the sense that the corresponding anion is strongly stabilized by resonance. However, in contrast with the assumption of Bordwell and Satish, our theoretical calculations seems to indicate that this resonance involves essentially the C3−C4−C5−C6−C7 skeleton, with a quite small participation of both oxygen atoms.

As far as the basicity of tropolone is concerned there are also some illustrative comparisons which can be made. Tropolone is found to be significantly more basic than benzoic acid.[37] This reflects, among other things, the high stability of the corresponding cation, already discussed in previous sections. At the same time tropolone is slightly less basic than tropone.[36] This result is a direct consequence of the chelation in the former compound, which contributes to decrease the basicity of the carbonyl oxygen atom, which behaves as a hydrogen bond acceptor. It can be argued, however, that this intramolecular hydrogen bond remains in the protonated species, but as we have discussed in previous sections, a topological analysis of the charge densities shows it to be weaker than that found in the neutral species. From the energetic point of view it is possible to have an estimation of this effect by comparing the relative stabilities of the two possible protonated forms, the *cis-trans* (**1H$^+$**) and the *trans-trans* (**1H$^+$tt**), with respect to the relative stabilities of the *cis* and *trans* forms of the neutrals. As reported by Sanna et al.[21] the energy difference between the *cis* and *trans* conformers of tropolone at the MP2/6-31G* level is 55 kJ/mol (13.1 kcal/mol). At the same level of accuracy, we have found that the energy difference between the *trans-trans* and the *cis-trans* conformers of protonated tropolone is only 21 kJ/mol (5.0 kcal/mol), which ratifies that the hydrogen bond in the protonated species is much weaker than in the neutral.

Conclusions

We have reported for the first time the basicity and acidity of tropolone in the gas phase. There is good agreement between the experimental values and the theoretical estimations obtained by means of *ab initio* calculations. This can be taken as an indication of the reliability of the level of theory used to describe the effects that protonation and deprotonation have on the aromaticity and on the overall stabilities of the neutral and charged systems. Our analysis shows that both the protonated and the deprotonated species are stabilized by resonance. As a consequence the acidity of tropolone is enhanced and tropolone is found to be surprisingly as acid as benzoic acid. This conclusion is in good agreement with the results obtained in DMSO[23] solutions. However, this agreement must be taken with caution. DMSO is a solvent particularly suited to stabilize ions due to its high dielectric constant and its high polarizability. Furthermore, it usually behaves as a good hydrogen bond acceptor. Hence, taking into account that benzoic acid is not chelated in the gas phase, the similar behavior observed for benzoic acid and tropolone as acids in the gas phase and in DMSO solutions might hide quite significant solvation effects in the latter case.

As far as the intrinsic basicity of tropolone is concerned we have found that its intramolecular hydrogen bond becomes weaker upon protonation, and this effect tends to counterbalance the resonance stabilization of the cation. As a consequence tropolone is found to be slightly less basic than tropone.

Acknowledgment. This work has been partially supported by the DGICYT Projects PB93-0286-C02 and PB93-0142-C03.

JO962161K

---

(37) *NIST Standard Reference Database 19B, NIST Negative Ion Energetics Database, Computerized Version 3.01*; National Institute of Standards and Technology: Gaithersburg, MD 20899, 1993.